Estimation of the Daytime and Nighttime Distribution of Atmospheric Ozone from Ground-Based Millimeter Wavelength Measurements

F. I. SHIMABUKURO, P. L. SMITH[1] AND W. J. WILSON

The Ivan A. Getting Laboratories, The Aerospace Corporation, Los Angeles, Calif. 90009

(Manuscript received 15 February 1977, in revised form 8 July 1977)

ABSTRACT

The daytime and nighttime distribution of the ozone density in the atmosphere has been determined from ground-based measurements of the emission spectra of the strong $4_{0,4}=4_{1,3}$ rotational line of ozone at 101.737 GHz ($\lambda=2.9$ mm), using a least-squares parameter estimation technique. The inversion procedure is described, and a linearized model is used to obtain approximate error bounds on the ozone parameter estimates.

1. Introduction

In a previous paper (Shimabukuro *et al.*, 1975), the ozone distribution in the atmosphere was estimated from millimeter wavelength spectral line absorption measurements of the $6_{0,6}$-$6_{1,5}$ rotational line of O_3 at 110.836 GHz, using the sun as a source. Since then, a more sensitive spectral line receiver was developed at The Aerospace Corporation (Wilson *et al.*, 1976), and using this receiver, the ozone distribution can now be estimated from emission measurements of atmospheric ozone. Emission measurements at 110.8 GHz from mesospheric O_3 have been reported by Penfield *et al.* (1976). In this paper the technique of obtaining the ozone density from the emission profile of the $4_{0,4}$-$4_{1,3}$ rotational line of O_3 at 101.737 GHz is briefly described, and observations of the nighttime enhancement of mesospheric O_3 is reported. In the inversion procedure, the parameters of an ozone density model are estimated from the measured emission spectrum. A linearized model is used to obtain approximate error bounds on the derived ozone parameter estimates. The radio technique for determining the ozone density distribution is a potentially valuable tool in atmospheric research, and can be used to monitor the long and short term variation of O_3 from ground-based sites for local coverage and from satellites for global coverage.

2. Measurements

The ozone emission measurements were made on 27–28 January 1976 using the Aerospace 4.6 m antenna and millimeter wave spectral line receiver, located in El Segundo, Calif. (latitude 34°N, altitude 38 m). A superheterodyne mixer receiver was used and, at the observation frequency of 101.737 GHz, the system noise temperature was measured to be ~500 K (double side band), using ambient and liquid nitrogen temperature loads. All measured antenna temperatures were calibrated against the system noise temperature. The emission spectrum of O_3 was measured with a filter spectrometer which had 64 channels with 1 MHz resolution and 64 channels with 0.25 MHz resolution. Real-time processing of the data was done with a NOVA 800 minicomputer system and plots of the ozone spectrum were obtained hourly. The atmospheric continuum attenuation, due to water vapor and oxygen, was determined by measuring the atmospheric emission temperature at several zenith angles. During the course of the measurements, the continuum absorption τ_c was in the range 0.08–0.09. For maximum signal, the O_3 emission measurements were made at a zenith angle determined by the relation $\tau_c \sec z=1$. All measurements were corrected for the continuum atmospheric attenuation, the antenna beam efficiency (0.95), and normalized to the zenith ($\sec z=1$). The observations were made using the frequency switched mode of operation to reduce the systematic baseline curvature. Although this technique removed most of the baseline curvature, it was still necessary to correct for a small linear baseline drift. In the frequency switched mode of operation the local oscillator is periodically switched (10 Hz) between two frequencies and the output spectrum is the difference of two signals. The measured profile is

$$z(\nu)=z'(\nu)-z'(\nu+\nu_s)+B(\nu), \qquad (1)$$

where $z'(\nu)$ is the unswitched profile, ν_s the switching frequency interval, and $B(\nu)$ the residual baseline curvature not removed by the frequency switching

[1] Guidance and Control Division, The Aerospace Corporation, Los Angeles.

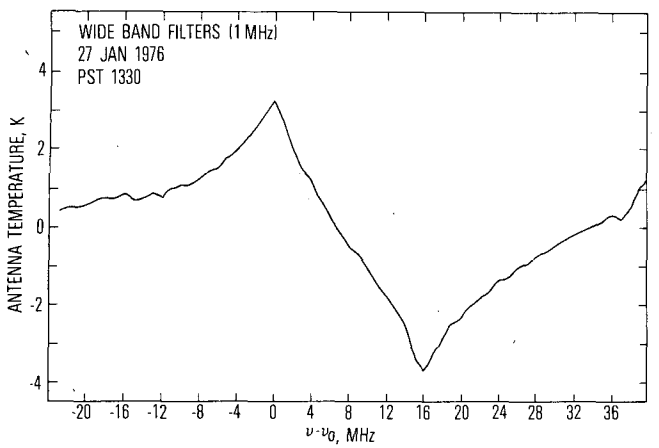

FIG. 1. Measured frequency-switched emission profile of atmospheric O_3 at $\nu_0=101.737$ GHz, using 1 MHz bandwidth filters.

process and is caused by the fact that the receiver gain is not identical at ν and $\nu+\nu_s$, and varies with time. A typical measured spectrum with the wideband 1 MHz filters is shown in Fig. 1. One of the advantages of frequency switching is that the baseline is accurately located (halfway between the peaks in Fig. 1) and measurements far out in the wings of the line are not required to determine it. The emission profiles measured with the narrowband 0.25 MHz filters are shown in Fig. 2 at different times of the day. Notice the nighttime enhancement of mesospheric O_3 in the central channels.

3. Formulation

The emission spectrum $s(\nu)$ at frequency ν, normalized to the zenith, is given by

$$s(\nu)=\int_{h_0}^{\infty} T(h)\exp\left[-\int_{h_0}^{h}\alpha(\nu,h')dh'\right]\alpha(\nu,h)dh, \quad (2)$$

where $T(h)$ is the temperature, h_0 the altitude of the observing site, $\alpha(\nu,h)$ the absorption coefficient and h the height. From Gora (1959) and Townes and Schawlow (1955) the absorption coefficient for the $4_{0,4}$-$4_{1,3}$ line is

$$\alpha(\nu,h)=\frac{3.91\times10^{-24}N(h)\nu^2e^{-12.1/T(h)}}{T(h)^{\frac{3}{2}}}f(\nu,h)\ [\mathrm{km}^{-1}], \quad (3)$$

where $N(h)$ is the ozone density in molecules per cubic centimeter, ν the frequency in hertz, and $f(\nu,h)$ the normalized line shape function. Since the emission measurements are sensitive to ozone in the lower atmosphere, where pressure broadening predominates, to the mesosphere, where Doppler broadening is dominant, the Voigt profile is used throughout, which is given by

$$f(\nu,h)=\frac{1}{\Delta\nu_D}\left(\frac{\ln 2}{\pi}\right)^{\frac{1}{2}}\frac{y}{\pi}\int_{-\infty}^{\infty}\frac{e^{-t^2}dt}{y^2+(x-t)^2}, \quad (4)$$

where $y=(\Delta\nu_C/\Delta\nu_D)(\ln 2)^{\frac{1}{2}}$, $x=[(\nu-\nu_0)/\Delta\nu_D](\ln 2)^{\frac{1}{2}}$, ν_0 is the rest frequency, 101.737×10^9 Hz, $\Delta\nu_C=5.28\times10^7P(h)T(h)^{-\frac{1}{2}}$ Hz (Walshaw, 1955), $P(h)$ is the total pressure (torr), and

$$\Delta\nu_D=\frac{\nu_0}{c}\left[\frac{2kT(h)}{m}\ln 2\right]^{\frac{1}{2}}=5240T(h)^{\frac{1}{2}}\ [\mathrm{Hz}]$$

for O_3. The procedure outlined by Armstrong (1967) was used to compute the Voigt function. The temperature and pressure distribution used are the values of the *U. S. Standard Atmosphere* (1962).

The model relating the ozone density to the measured emission spectrum at frequency ν_k is

$$z(\nu_k)=(1/\mathrm{BW})\int_{\nu_k-\frac{1}{2}\mathrm{BW}}^{\nu_k+\frac{1}{2}\mathrm{BW}}[s(\nu)-s(\nu+\nu_s)]d\nu+W(k), \quad (5)$$

where $W(k)$ is the measurement error and BW the filter bandwidth.

The determination of $N(h)$ from the measured spectra involves the inversion of Eq. (2) which is an integral equation. A parametric model for the ozone density was assumed. By doing this, unique parameter estimates can be obtained without any prior assumptions about the parameter values, and standard optimization methods and error analysis techniques can be used. The calculated $N(h)$ is accurate to the extent that the parametric model can fit the actual density distribution. More complex parametric models can be fitted to the measurements, but the number of parameters which can be uniquely determined ultimately depends on the number of independent measurements and the quality of the data.

The model chosen for the ozone density is given by

$$N(h)=\frac{4D_m\exp[r_m(h-h_m)]}{\{1+\exp[r_m(h-h_m)]\}^2}+D_p\exp[-r_p^2(h-h_p)^2]. \quad (6)$$

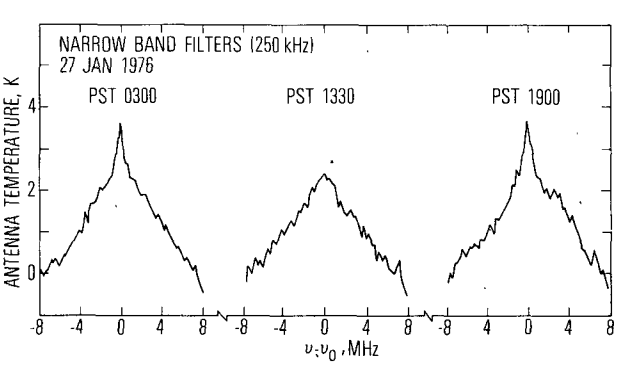

FIG. 2. Measured frequency-switched emission profiles of atmospheric O_3 using 0.25 MHz bandwidth filters, taken at different times of the day (Pacific Standard Time).

The first term on the right-hand side of Eq. (6) is similar to the model proposed by Green (1964). The second term is the expression for the secondary peak due to the nighttime enchancement of O_3 in the mesosphere and the Gaussian shape has been found to be representative of the ozone density (Roble and Hays, 1972). The parameters which determine the shape of the model ozone distribution are as follows:

- D_m density of the primary peak located in the 15–30 km region (mol cm^{-3})
- h_m altitude of the primary peak (km)
- r_m shape factor (km^{-1})
- D_p density of the secondary peak located in the 60–90 km region (mol cm^{-3})
- h_p altitude of the secondary peak (km)
- r_p shape factor (km^{-1}).

The total ozone content in a vertical column above the receiver is

$$\mathrm{TOC}=\int_{h_0}^{\infty} N(h)dh=\frac{4D_m}{r_m}\{1+\exp[r_m(h_0-h_m)]\}^{-1}. \quad (7)$$

The contribution from the secondary peak has been ignored because D_p is typically three or more orders of magnitude less than D_m.

Because of slight gain changes in the receiver system, there was a small baseline curvature in the output spectrum as discussed previously. The residual baseline curvature was approximated by a straight line. The measured output model is then given by

$$z(\nu_k)=t(\nu_k)-a(\nu_k-\nu_0)-b, \quad (8)$$

where $t(\nu_k)$ is the unprocessed antenna temperature at frequency ν_k, a is the slope of the baseline and b the bias offset. The parameters a and b adjust the tilt of the baseline slightly and have little effect on the basic calibration scale. The calibration is determined by the wide band measurements, shown in Fig. 1. The errors in these parameters are small and have a negligible effect on the ozone parameter estimates. From Eqs. (6) and (8) it is seen that there are six ozone and two baseline parameters to be determined. The measurements are sensitive to only four of six ozone parameters: D_m, r_m, h_m and D_p. The measurements are not sensitive to r_p and h_p because the secondary peak occurs in the mesosphere where Doppler broadening becomes significant, and no information about the height distribution can be obtained from the measured line profile. Only the center filter channel is sensitive to the mesospheric O_3 and then only to the integrated distribution. The parameters r_p and h_p were assigned the values suggested by Roble and Hays (1972), $h_p=83$ km, and $r_p=0.2$ km^{-1}.

TABLE 1. Estimate of ozone parameters.

Parameter	Local standard time 0300	1300	1900
D_m (mol cm^{-3})	4.89×10^{12}	4.90×10^{12}	4.90×10^{12}
h_m (km)	21.8	21.8	21.8
r_m (km^{-1})	0.219	0.227	0.219
D_p (mol cm^{-3})	1.06×10^{9}	-0.01×10^{9}	1.11×10^{9}
TOC (mol km cm^{-3})	88.4×10^{12}	85.5×10^{12}	88.4×10^{12}

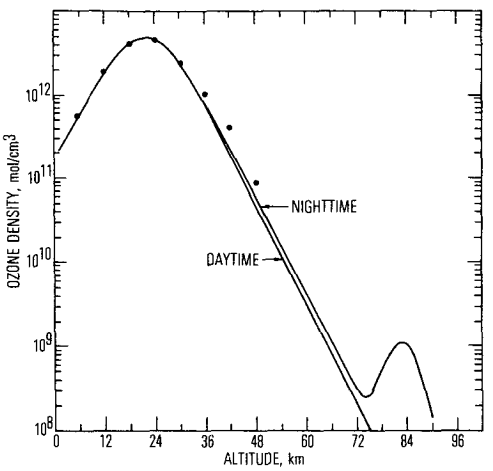

FIG. 3. Estimated daytime and nighttime distributions of atmospheric O_3 for the parametric ozone model. The dots are values for a mid-latitude ozone model. (see text).

The parameters to be estimated from the frequency differenced emission measurements are the four sensitive ozone density parameters, D_m, h_m, r_m, D_p and the two baseline parameters a and b. We define the parameter vector $\boldsymbol{\theta}$ as

$$\boldsymbol{\theta}=\begin{bmatrix} D_m \\ h_m \\ r_m \\ D_p \\ a \\ b \end{bmatrix}. \quad (9)$$

The least-squares estimate of $\boldsymbol{\theta}$ is obtained by minimizing

$$F(\boldsymbol{\theta})=\sum_{k=1}^{M}\left\{t(\nu_k)-a(\nu_k-\nu_0)-b-(1/\mathrm{BW})\int_{\nu_k-\frac{1}{2}\mathrm{BW}}^{\nu_k+\frac{1}{2}\mathrm{BW}}[s(\nu)-s(\nu+\nu_s)]d\nu\right\}^2, \quad (10)$$

where M is the number of measurements.

Davidon's numerical optimization technique (Fletcher and Powell, 1963) was used to find the value of $\boldsymbol{\theta}$ which minimized $F(\boldsymbol{\theta})$. The integrals were approximately by finite sums in increments of 1 km in altitude up to 90 km, and in increments of 0.025 MHz in frequency. The estimated values of the O_3 parameters at three different times of the day are shown in Table 1. Plots of the calculated daytime and nighttime O_3 distributions are shown in Fig. 3. The dots on the graph are the values

for a mid-latitude ozone model (*U. S. Standard Atmosphere Supplements*, 1966).

4. Error analysis

One advantage of least-squares parameter estimation is that no knowledge of the statistical properties of the measurement errors is required in order to apply the technique. To determine approximate error bounds on the least-squares estimates of the ozone parameters, a linearized measurement model was derived and assumptions were made about the statistical properties of the measurement error. Eq. (5) is rewritten as

$$z(\nu_k)=g_k(\boldsymbol{\theta})+W(k), \tag{11}$$

where

$$g_k(\boldsymbol{\theta})=(1/\mathrm{BW})\int_{\nu_k-\frac{1}{2}\mathrm{BW}}^{\nu_k+\frac{1}{2}\mathrm{BW}}[s(\nu)-s(\nu+\nu_s)]d\nu. \tag{12}$$

The linearized measurement model is obtained by expanding Eq. (11) in a Taylor series about the least-squares estimate $\boldsymbol{\theta}=\hat{\boldsymbol{\theta}}$:

$$z(\nu_k)=g_k(\boldsymbol{\theta})+\frac{\partial g_k(\boldsymbol{\theta})}{\partial D_m}(D_m-\hat{D}_m)+\frac{\partial g_k(\boldsymbol{\theta})}{\partial h_m}(h_m-\hat{h}_m)+\frac{\partial g_k(\boldsymbol{\theta})}{\partial r_m}(r_m-\hat{r}_m)+\frac{\partial g_k(\boldsymbol{\theta})}{\partial D_p}(D_p-\hat{D}_p)+\text{higher order terms}+W(k), \tag{13}$$

where $g_k(\boldsymbol{\theta})$ and its partial derivatives are evaluated at $\boldsymbol{\theta}=\hat{\boldsymbol{\theta}}$. The vector $\mathbf{x}$ is defined to contain the ozone parameter errors, i.e.,

$$\mathbf{x}=\begin{bmatrix} D_m-\hat{D}_m \\ h_m-\hat{h}_m \\ r_m-\hat{r}_m \\ D_p-\hat{D}_p \end{bmatrix}. \tag{14}$$

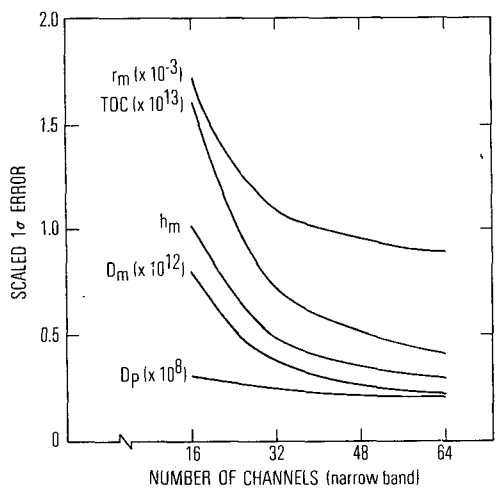

FIG. 4. Linearized standard errors for the estimated ozone parameters and for the total ozone content (TOC), as a function of the number of channels in the spectrometer used in the estimation process.

Ignoring the higher order terms, Eq. (13) can be written as a linear regression equation

$$z(\nu_k)-g_k(\boldsymbol{\theta})=H_k\mathbf{x}+W(k), \tag{15}$$

where H_k is the matrix of partial derivatives of the measurement model evaluated at $\boldsymbol{\theta}=\hat{\boldsymbol{\theta}}$:

$$H_k=\left[\frac{\partial g_k(\boldsymbol{\theta})}{\partial D_m}\ \frac{\partial g_k(\boldsymbol{\theta})}{\partial h_m}\ \frac{\partial g_k(\boldsymbol{\theta})}{\partial r_m}\ \frac{\partial g_k(\boldsymbol{\theta})}{\partial D_p}\right]_{\boldsymbol{\theta}=\hat{\boldsymbol{\theta}}}. \tag{16}$$

The partial derivatives are computed numerically by finite-difference techniques.

The error $W(k)$ is assumed to be random with zero mean and variance σ^2. The 4×4 error covariance matrix $\mathbf{P}$ for the ozone parameter estimates is

$$\mathrm{cov}(\mathbf{x})\equiv\mathbf{P}=\sigma^2\Big[\sum_{k=1}^{M}H_kH_k^{\mathrm{T}}\Big]^{-1}. \tag{17}$$

Eq. (17) is a standard result in linear regression analysis (Wilks, 1962). The square roots of the diagonal element of $\mathbf{P}$ are the approximate standard (one sigma) errors in the ozone parameter estimates.

The approximate estimation error in the total ozone constant is obtained by the same linearization technique. The approximate covariance of the estimation error in $\widehat{\mathrm{TOC}}$ is

$$\mathrm{cov}(\mathrm{TOC}-\widehat{\mathrm{TOC}})=\mathbf{S}^{\mathrm{T}}\mathbf{P}\mathbf{S}, \tag{18}$$

where

$$\mathbf{S}^{\mathrm{T}}=\left[\frac{\partial\,\mathrm{TOC}(\boldsymbol{\theta})}{\partial D_m}\ \frac{\partial\,\mathrm{TOC}(\boldsymbol{\theta})}{\partial h_m}\ \frac{\partial\,\mathrm{TOC}(\boldsymbol{\theta})}{\partial r_m}\ \frac{\partial\,\mathrm{TOC}(\boldsymbol{\theta})}{\partial D_p}\right]_{\boldsymbol{\theta}=\hat{\boldsymbol{\theta}}}.$$

The partial derivatives can be calculated analytically from Eq. (7). In Fig. 4 are shown the standard errors calculated by this method for a filter bandwidth of 0.25 MHz, utilizing a different number of filter channels in the estimation process. There is not a dramatic reduction in the standard error by increasing the spectrometer bandwidth beyond 32 narrow-band channels (8 MHz) and this factor has to be considered in the design of an efficient ozone spectrometer. For example, the standard errors for D_m, r_m, h_m, D_p and TOC are 7, 2, 0.5, 2.3 and 8%, respectively, when data from 32 channels centered about ν_0 are used in the analyses, and, when 64 channels are used, the errors are reduced to 5, 1.4, 0.4, 2 and 5%. It has been assumed in this discussion that there are no unmodeled systematic errors. Only the effects of random errors are shown in the plot.

5. Discussion of results

The radio technique, using emission measurements, is effective for estimating the parameters of the assumed ozone model. The estimated O_3 distribution is in the range of what might be expected, up to an altitude

of 60 km, as shown in Fig. 3. The radio measurements are sensitive to the increased nighttime O_3 above 60 km, but not to its distribution. For assumed values of $h_p = 83$ km, $r_p = 0.2$ km^{-1}, D_p is estimated to be 1.1×10^9 mol cm^{-3}, which is comparable to the value of 8×10^8 mol cm^{-3} reported by Roble and Hays (1972). If the altitude of the secondary peak is assumed to occur elsewhere, the estimated peak density changes accordingly. For example, in Fig. 5 are shown plots of the estimated nighttime O_3 density for three assumed height locations of the secondary peak for $r_p = 0.2$ km^{-1}.

Further insight into the radio technique can be obtained by examining the equation of radiative transfer, i.e.,

$$z(\nu_k) = \int_{h_0}^{\infty} (1/\mathrm{BW}) \int_{\nu_k - \frac{1}{2}\mathrm{BW}}^{\nu_k + \frac{1}{2}\mathrm{BW}} T(h) \times \exp\left[-\int_{h_0}^{h} \alpha(\nu,h')dh' \right] \alpha(\nu,h) dh d\nu. \quad (19)$$

Eq. (19) can be rewritten as

$$z(\nu_k) = \int_{h_0}^{\infty} N(h) d_k(h) dh, \quad (20)$$

where

$$d_k(h) = (1/\mathrm{BW}) \int_{\nu_k - \frac{1}{2}\mathrm{BW}}^{\nu_k + \frac{1}{2}\mathrm{BW}} T(h) \times \exp\left[-\int_{h_0}^{h} \alpha(\nu,h')dh' \right] \alpha(\nu,h) N(h)^{-1} d\nu.$$

The exponential term is approximately constant so that in the discussion to follow, $d_k(h)$ can be regarded as the weighting function for the filter located at frequency ν_k. Plots of $d_k(h)$ at different filter frequencies are shown in Fig. 6 for a filter bandwidth of 0.25 MHz.

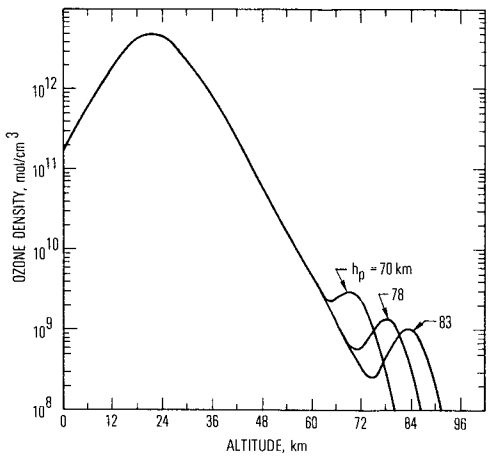

FIG. 5. Estimated nighttime O_3 distribution for three assumed altitudes for the secondary peak.

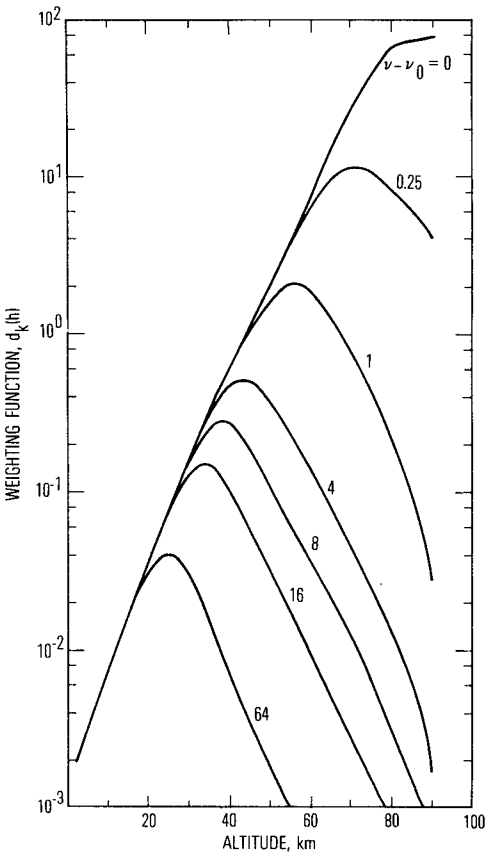

FIG. 6. Weighting functions for 0.25 MHz bandwidth filters located at various frequencies (MHz) away from line center.

The weighting functions show a varying sensitivity as a function of altitude and frequency. The nighttime increase of mesospheric ozone can be detected, even though the peak density there is several orders of magnitude less than the primary peak, because the weighting function of the central channel increases with altitude. The sensitivity to the secondary peak would have been increased if a narrower band filter at the center channel had been used. At frequencies further away from the rotational line frequency, the sensitivity decreases, and the behavior of the estimation errors, plotted in Fig. 4, is apparent. The capabilities and limitations of the radio technique, and the design of an efficient ozone spectrometer will be investigated in detail in a later paper.

Acknowledgments. The authors would like to express their gratitude to J. D. White and M. V. Wright, who helped make the measurements, and to E. R. Coffey who assisted in the mathematical computations.

This work was supported by The Aerospace Corporation.

REFERENCES

Armstrong, B. H., 1967: Spectrum line profiles: The Voigt function. *J. Quant. Radiat. Transfer*, **7**, 61–88.

Fletcher, R., and M. J. D. Powell, 1963: A rapidly convergent descent method for minimization. *Comput. J.*, **6**, 163–168.

Gora, E. K., 1959: The rotational spectrum of ozone. *J. Mol. Spectrosc.*, **3**, 78–99.

Green, A. E. S., 1964: Attenuation by ozone and the earth's albedo in the middle ultraviolet. *Appl. Opt.*, **3**, 203–208.

Penfield, H., M. M. Litvak, C. A. Gottlieb and A. E. Lilley, 1976: Mesospheric ozone measured from ground-based millimeter-wave observations. *J. Geophys. Res.*, **81**, 6115–6120.

Roble, R. G., and P. B. Hays, 1972: A technique for recovering the vertical number density profile of atmospheric gases from planetary occultation data. *Planet. Space Sci.*, **20**, 1727–1744.

Shimabukuro, F. I., P. L. Smith and W. J. Wilson, 1975: Estimation of the ozone distribution from millimeter wavelength absorption measurements, *J. Geophys. Res.*, **80**, 2957–2959.

Townes, C. H., and A. L. Schawlow, 1955: *Microwave Spectroscopy*. McGraw-Hill, 608 pp.

U. S. Standard Atmosphere, 1962: Govt. Printing Off., Washington, D. C.

U. S. Standard Atmosphere Supplements, 1966: Govt. Printing Off., Washington, D. C.

Walshaw, C. D., 1955: Line widths in the 9.6-μ band of zone. *Proc. Phys. Soc. London*, **A68**, 530–534.

Wilks, S., 1962: *Mathematical Statistics*. Wiley, 644 pp.

Wilson, W. J., R. L. Dickman, G. G. Berry, E. H. Erfurth, H. B. Dyson, T. T. Mori, H. E. King and J. D. White, 1976: The Aerospace millimeter-wave spectral line receiver. Aerospace Rep. ATR-76(8201)-1.